International Journal of Environmental Science and Technology (2022) 19:10257–10274
https://doi.org/10.1007/s13762-021-03847-5

ORIGINAL PAPER

Exploring land use/land cover change by using density analysis method in yenice

H. Aksoy[1] · S. Kaptan[2] · T. Varol[2] · M. Cetin[3] · H. B. Ozel[2]

Received: 21 September 2021 / Revised: 25 November 2021 / Accepted: 6 December 2021 / Published online: 26 January 2022

Abstract

In this study, the changes in forest areas and land cover in the period of 2001–2011 and 2011–2021 in the Yenice Forestry Operation Directorate of Turkey were examined in time interval, category and transition levels by using the density analysis method. Landsat images of the study area for the relevant years were classified according to the supervised classification method, land cover change maps and matrices were produced. Method of Intensity Analysis dissects the transition matrices of 2001–2011 and 2011–2021 time period for six categories: Coniferous, Broad-Leaved, Mixed, Settlement, Agriculture and Water. Interval results of the analysis show that the accelerated change in the second period resulted in a decrease in mixed forest and agricultural areas (2%, 8%, respectively) and an increase in residential and pure forests (1% and 9%, respectively) in 20 years. According to the category level results, Broad-Leaved category is active in gain in the first time interval and dormant in terms of loss and gain in the second time interval. Mixed, on the other hand, is an active loser in the first timeframe and active in terms of gains in the second timeframe. According to the Transition level results, the gains of Coniferous and Mixed categories showed that they targeted each other's losses in both time intervals. While Broad-Leaved targeted Mixed losses in the first timeframe, Agriculture losses were targeted as gains in the second timeframe.

Keywords Land classification · Landsat imagery · Remote sensing · Turkey

Introduction

Emerging as a result of the complex relationships between humans and the physical environment (Sarma et al. 2008; Manandhar et al. 2010; Huang et al. 2012), showing effects in many areas from biodiversity to climate, health to economy (Foley et al. 2005; Shafizadeh-Moghadam 2019) land use and land cover changes (LULC) are recognized as one of the most important environmental issues globally (Halmy et al. 2015). Generally, LULC change begins as a result of anthropogenic effects, followed by natural processes (Niemelä et al. 2000; Srivastava et al. 2012; Singh et al. 2015). LULC changes, which occur with the effect of human-induced activities as the driving force, show their effect faster and more severely compared to the changes triggered by natural events. Empirical studies conducted by many researchers from different disciplines have revealed that LULC changes are the key to various applications such as forest, environment, agriculture, geology, hydrology, ecology (Weng 2001; Hassan 2016; Twisa and Buchroithner 2019).

Since the changes in LULC change the structure and functions of ecosystems, they directly or indirectly affect ecosystem services (Han et al. 2016; Peng et al. 2015; Song and Liu 2017; Guo et al. 2021). The energy crisis that emerged with the industrial revolution and the rapid increase in the world population have adversely affected forest areas and resources and continue to do so. In particular, forest degradation or deforestation has brought along many ecological, economic and social problems such as global warming, loss of biodiversity, hydrological losses, erosion, habitat

Editorial responsibility: Maryam Shabani.

M. Cetin
mcetin@kastamonu.edu.tr

1 Vocational School of Ayancik, Department of Forestry, Program of Forestry and Forest Products, Sinop University, Sinop, Turkey

2 Department of Forest Engineering, Faculty of Forestry, Bartin University, Bartin, Turkey

3 Department of Landscape Architecture, Faculty of Engineering and Architecture, Kastamonu University, Kuzeykent Campus, 37150 Kastamonu, Turkey

degradation, slowing down or regression of benefiting from the products and services offered by the forest ecosystem.

The historical, continuous and precise information to be obtained about the global LULC changes is very important for many sustainable development programs in which LULC is a core element (Abd El-Kawy et al. 2011) or for taking necessary measures to prevent the reduction in natural resources (Kindu et al. 2015; Salem et al. 2020). Understanding the causes and consequences of the current LULC changes, researching the place and scope of possible changes for the coming years has attracted the attention of many researchers from different disciplines (Aksoy and Kaptan 2020). Particularly in the last 20 years, the monitoring of the LULC change has become an irreplaceable monitoring that attracts attention not only in Europe but also all over the world (Manakos and Braun 2014; Gadrani et al. 2018). In many studies in which LULC changes are measured and monitored, remote sensing (RS) and geographic information systems (GIS) are widely preferred because of their advantages such as low cost, short data generation capability, and working in harmony (Varol and Yılmaz 2006; Acheampong et al. 2018; Barakat et al. 2019; Tadese et al. 2020; Paul et al. 2021). In addition, the increase in the number of satellite images with the developing technology has facilitated the production of LULC maps in large areas and at regular intervals (Friedl et al. 1999; Zeng et al. 2010; Nyamekye et al. 2020).

The terrain transition matrix (Duan et al. 2021), which is one of the most widely used methods for detecting LULC changes, is produced by overlaying LULC images from different years produced by classification of satellite images. However, the interpretations made by the direct evaluation of these tables are insufficient to explain the change processes and reasons between the land categories (Huang et al. 2012; Kaptan 2021). Aiming to eliminate this deficiency, Aldwaik and Pontius (2012) developed a density analysis consisting of three levels: interval level, category level and transition level, which includes some calculations. In this way, they aimed to interpret the processes of temporal and spatial changes between LULC categories. Density analysis, which goes beyond mapping to measure the temporal and spatial dynamics of LULC change, has attracted the attention of many researchers from different parts of the world (Zhou et al. 2014; Berakhi 2015; Yang et al. 2017; Huang et al. 2018; Varga et al. 2019; Sun et al. 2021). Analysis can offer the opportunity to evaluate the valid evidence of a particular change process, as well as assist in the development of new hypotheses related to these processes (Aldwaik and Pontius 2013; Huang et al. 2018; Kaptan 2021).

The studies on LULC changes at the scale of Turkey generally evaluated the changes between land categories and their amounts without including any calculations, based on the results they obtained from traditional land change matrices. Focusing on the temporal and spatial changes of forest dynamics, Bozali et al. (2015), Kaptan and Durkaya (2019), Çoban and Gündoğdu (2020), Aksoy and Kaptan (2020), it was determined that there was an increase in forest areas according to the results of classical change matrices. According to the Food and Agriculture Organization of the United Nations (FAO) report published in 2020, Turkey ranks 6th among the countries with the highest annual net forest income in the 2010–2020 period (FAO 2020).

In this study, which investigates the changes in forest and land cover in the Yenice district of Karabük, Turkey, between 2001–2011 and 2011–2021, and the reasons for these changes, it has been developed by Aldwaik and Pontius (2012, 2013), including interval level, category level and transition level. A three-level density analysis was used. Although it is possible to come across some LULC studies using density analysis in the international arena, no study using density analysis has yet been found in Turkey. As far as it is known, this study is the first article in which density analysis was used among LULC studies conducted in in the Yenice district of Karabük, Turkey, 2021.

The change matrix tables containing the data forming the input of the density analysis performed for 6 categories as coniferous, broad-leaved, mixed, settlement, agriculture and water were produced by using RS (Landsat images) and GIS (ENVI and ArcGIS) tools together. In the study, the temporal and spatial changes experienced in each category from 2001 to 2021 and the transitions between the categories were interpreted with the graphics presented by the analysis, and the driving forces and scopes of these changes were attempted to be understood.

Materials and methods

Study area

In these study of material was conducted in the Yenice district of Karabük, Turkey which is the coordinates of 41°10' 48'' N and 32° 20''' E is located in the western Black Sea region in showing Fig. 1. Due to its geographical structure, the district has very rough terrain and very dense forest areas. In its forests, there are monumental trees and a large number of tree species that have reached a height and diameter well above the standards. It also has uninterrupted forests in which there are no settlements, called the "forest sea" (OGM 2021).

Data and materials

Landsat-7 ETM+(Enhanced Thematic Mapper Plus) and Landsat-8 OLI/TIRS (Operational Land Imager/Thermal Infrared) downloaded from the United States Geological

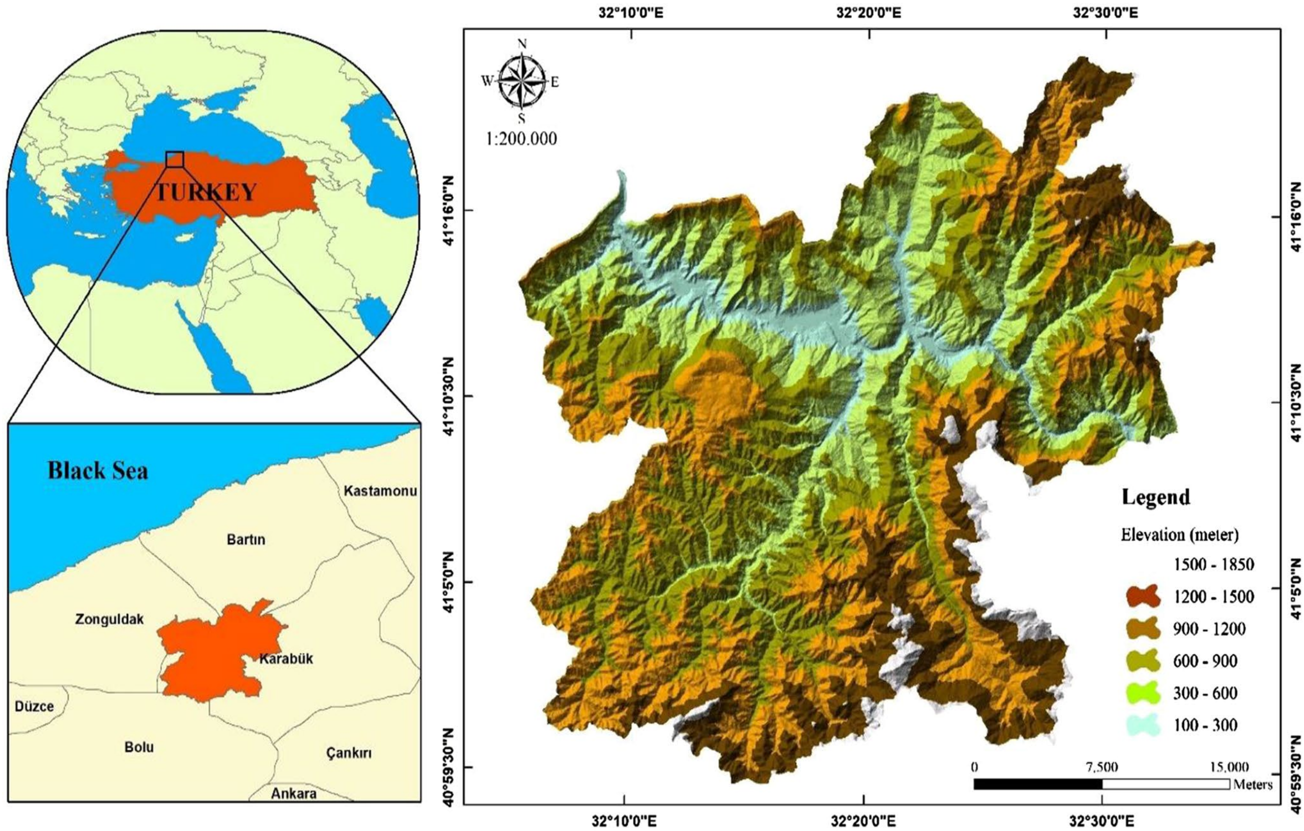

Fig. 1 Location map of the study area

Survey (USGS 2021) website for the production of land cover and use maps for 2001, 2011 and 2021. Sensor) satellite images were used. Classification processes and accuracy calculations of satellite images classified by the supervised classification method were performed using ENVI software. In the classification process, forest cover types maps were used as reference data. Land use and cover maps are arranged to show 6 categories: coniferous, broad-leaved, mixed, settlement, agriculture and water. The flowchart showing the general methodological framework of the study is shown in Fig. 2.

Image preprocessing and correction

Satellite images of the same season, cloudless (< 10%) and the years 2001, 2011 and 2021 were used to perform the classification at the highest level of accuracy of the research. The characteristics of the satellite images used are given in Table 1.

In order to distinguish land use classes with maximum accuracy, image enhancement (Pan Sharpening) was applied to satellite images as 1% standard deviation correction. In satellite images, some systematic errors may occur radiometrically in the image brightness values depending on the weather conditions at the time the image is taken, the position of the sun, the cloudiness rate, the sensor, the wavelength of the reflection, atmospheric and topographic effects. In order to minimize the lines in the study, the radiometric errors in the images were corrected with ENVI software so that the root mean square error (RMSE) was less than one pixel. Atmospheric corrections of the images were also performed using the same software.

According to the band characteristics of the satellite images used in the study, the composite band process was applied for each period. After the composite tape raster images were cut according to the study area, the image enhancement process was applied to the cut satellite images (Pan Sharpening). The main purpose of the image enrichment process performed on satellite images; to increase the perceptibility, interpretability, quality and quality of images. Depending on this method, it is aimed to increase the success rate of classification.

Identification of reference trial pixels and supervised classification

In the image classification process, two different classification methods are used, supervised and unsupervised. In

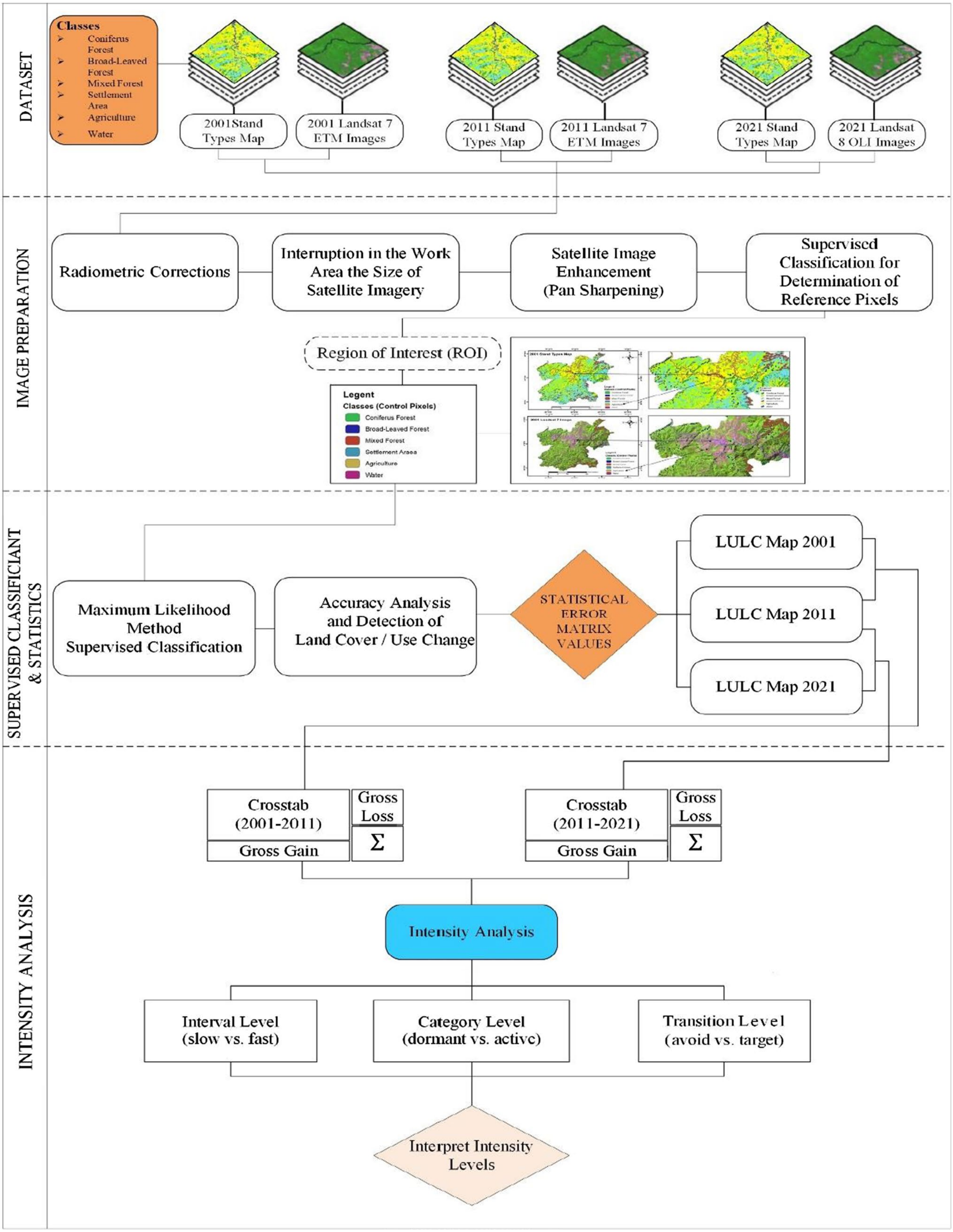

Fig. 2 Method flowchart

Table 1 Landsat satellite data and band (image) properties (USGS 2021)

Satellite	Date Acquired	Path	Row	Spectral Range	Wave length Range (µm)	Spatial Resolution (m)
Landsat 7 ETM+	30.06.2001 & 28.07.2011	177	31–32	Band 1	0.45 – 0.51	30
				Band 2	0.53 – 0.61	30
				Band 3	0.63– 0.69	30
				Band 4	0.75 – 0.90	30
				Band 5	1.55 – 1.75	30
				Band 6	10.4 – 12.5	30
				Band 7	1.09 – 2.35	30
				Pan	0.52 – 0.90	15
Landsat 8 OLI/TIRS	1.May.21	178	31	Band 1	0.43 – 0.45	30
				Band 2	0.45 – 0.51	30
				Band 3	0.53 – 0.59	30
				Band 4	0.64 – 0.67	30
				Band 5	0.85 – 0.88	30
				Band 6	1.57 – 1.65	30
				Band 7	2.11 – 2.29	30
				Band 8 (pan)	0.50 – 0.68	15

the unsupervised classification method, when there is no information about the image, classification is made by creating clusters according to the spectral reflection value of the image. In supervised classification, it refers to the situation of classification by reference to materials that have spatial and objective information about the image. In the study based on the stand types maps of the Yenice Forestry Operation Directorate (OIM- Forestry Operation Directorate) 2001, 2011 and 2021, trial pixels were created for each class and supervised classification was applied to the satellite images of the relevant years.

To create and analyze land use/maps, a total of six classification categories were defined: coniferous, leafy and mixed forest from the forest area class, and settlement, agriculture and water from the non-forest class. The reference points required for the supervised classification process were determined using stand type maps of 2001, 2011 and 2021, GPS data from terrestrial measurements and high resolution Google Earth images. Reference points were determined for each class according to the density and distribution of the classes in the field from the stand types map, terrestrial measurements (GPS) and Google Earth images. Snedecor and Cochran (1969) was used to determine the minimum number of sample points in the number of reference pixels taken (Eq. 1)

$$N = 4pq/E \tag{1}$$

N: Total number of pixels to sample. p: Expected percent accuracy. q: 100-p. E: Maximum allowed error percentage.

As a result of the calculations, the minimum number of sample pixels was determined as 3096 for an accuracy rate of 85% and a maximum margin of error of 5%. Then, the reference pixels were overlapped with the satellite image, and the satellite images were classified based on the reflectance values of the pixels corresponding to each trial group. The distribution of the reference points in the stand types map and satellite image is shown in Fig. 3.

The accuracy of the satellite image obtained as a result of supervised classification was checked using the error matrix method based on reference pixels. Accuracy evaluations of the images were determined. These; It consists of overall accuracy, producer's accuracy, user's accuracy and kappa statistics. General accuracy; how well the obtained classification result matches the actual situation in the field, manufacturer accuracy; how well each class is classified with example points, while user accuracy; it shows how many of the user's real situation points in the field are represented correctly on the classified map. Finally, the Kappa (κ) coefficient is a statistical indicator that expresses the real agreement between the reference data and the classified map (Aksoy and Kaptan 2020).

Land use and cover change matrix

In order to produce the change matrix showing the transitions between the land categories, the 2001, 2011 and 2021 LULC maps in raster format, which were produced as a result of the classification, were converted and saved as polygons in ArcGIS 10.8 software. For the 2001–2011 and 2011–2021 time intervals, the initial and last time maps were overlapped and saved with the "Intersect" command. Transition matrices showing the transitions and change

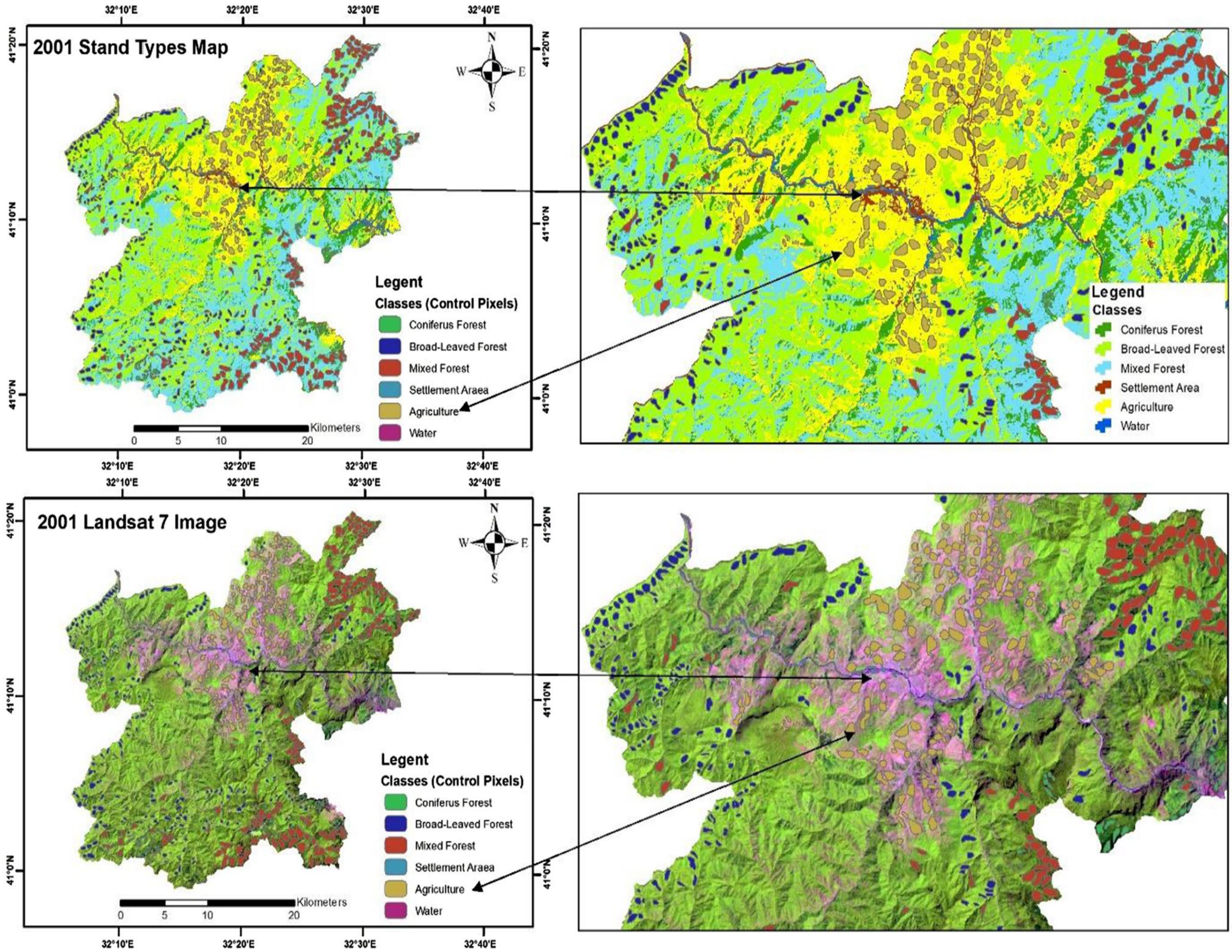

Fig. 3 Distribution of reference pixels

amounts between the categories in Excell with the data copied for a total of 6 categories: coniferous, broad-leaved, mixed, settlement, agriculture, water from the database of the new map produced. The rows of this cross-classification matrix show the categories at time 1 (T1) and the columns show the categories at time 2 (T2) (Table 2). The cells indicated by the dashed line are a classic conventional transition matrix. While the diagonal entries (P11, P22, Pii, …) in the table represent the part of the relevant category that remains unchanged between the time period (the amount of persistence), all entries outside the diagonal indicate the amount of transition from the "i" category to a different "j" category (Pontius et al. 2004).

Intensity analysis

Although it is possible to see the amount of changes in land use with traditional change matrices, a deeper investigation is needed to explain the link between patterns and processes in different classes (Zaehringer et al. 2015; Kourosh Niya et al. 2019). Density analysis enables the interpretation of the results of a number of calculations performed with the data in the transition matrix to determine the differences of a set of categories at multiple time points (Aldwaik and Pontius 2012, 2013; Quan et al. 2020). The basic logic of density analysis is based on the comparison of the intensity of the experienced changes with respect to the uniform density, which represents the situation when it is assumed to be evenly distributed across the entire temporal and spatial extent (Acheampong et al. 2018). Density analysis is important to know whether an observed transition from one category to another deviates from an apparently uniform process (Akinyemi 2017). The analysis gives the results of the dimensions and intensity of the transitions between categories at three different levels: time interval, category and transition level. Time interval analysis examines the overall

Table 2 Temporal variation matrix of land cover

T_1	T_2								Total T_1	Lost (L)
	Category 1	Category 2	…	Category *i*	…	Category *j*	…	Category J		
Category1	P_{11}	P_{12}	…	P_{1i}	…	P_{1j}	…	P_{1J}	P_{1+}	$P_{1+}—P_{11}$
Category2	P_{21}	P_{22}	…	P_{2i}	…		…	P_{24}	P_{2+}	$P_{2+}—P_{22}$
…	…	…	…	…	…	…	…	…	…	…
Category *i*	P_{i1}	P_{i2}	…	P_{ii}	…	P_{ij}	…	P_{iJ}	P_{i+}	$P_{i+}—P_{ii}$
…	…	…		…		…	…	…	…	…
Category *j*	P_{j1}	P_{j2}	…	P_{ji}	…	P_{jj}	…	P_{jJ}	P_{j+}	$P_{j+}—P_{jj}$
…	…	…	…	…	…	…	…	…	…	…
Category*J*	P_{J1}	P_{J2}	…	P_{Ji}	…	P_{Jj}	…	P_{JJ}	P_{J+}	$P_{J+}—P_{JJ}$
Total T_2	P_{+1}	P_{+2}	…	P_{+i}	…	P_{+j}	…	P_{+J}	*1*	
Gain (G)	$P_{+1}—P_{11}$	$P_{+2}—P_{22}$	…	$P_{+i}—P_{ii}$	…	$P_{+j}—P_{jj}$	…	$P_{+J}—P_{JJ}$		

change in each time interval by the size and rate of change over time intervals. According to the analysis, where the annual change area is calculated for each time interval, the result compares with a uniform rate of change (U), which expresses the assumption that all changes occurring over the entire time interval are evenly distributed over the entire landscape (Yang et al. 2017). The left side of the graph showing the analysis results shows the change dimensions, and the right side shows the annual change intensities (St). If the bars on the right of this graph extend to the right of the uniform line indicated by the dashed line, it indicates that the change is fast for the relevant time interval, and if it ends before the uniform line, the rate of change is slow. The annual variation intensity (St) observed for each time interval is calculated according to Eq. 2, and the uniform annual variation rate (U) covering the entire study time is calculated according to Eq. 3 (Aldwaik and Pontius 2012, 2013; Kaptan 2021).

where J = the number of categories; i = the index for a category at an initial time; j = the index for a category at a subsequent time; T = the number of time points; t = the index for a time point ranging from 1 to $T-1$; Y_t = the year at time point t; C_{tij} = the size of the area that transitions from category i at time Y_t to category j at time Y_{t+1}.

Category level calculates the annual gain density (Gtj) and loss density (Lti) of each category according to Eqs. 4 and 5, and the uniform density (St) calculated according to Eq. 2, which will occur if all categories gain or lose the same intensity in every time interval. compares with. If the annual change intensities of losses and gains for a certain time period for a category are greater than the uniform change intensity calculated for the relevant time period, it means that the category is active (active) in terms of loss and gain, and if it is small, it means that it is dormant.

$$S_t = \frac{\left(\text{area of change during interval}[Y_t, Y_{t+1}]\right) / \left(\text{area of study region}\right)}{\text{duration of interval}[Y_t, Y_{t+1}]} \times 100\% = \frac{\left\{ \sum_{j=1}^{J} \left[\left(\sum_{i=1}^{J} C_{tij} \right) - C_{tij} \right] \right\} / \left[\sum_{j=1}^{J} \left(\sum_{i=1}^{J} C_{tij} \right) \right]}{[Y_{t+1} - Y_t]} \times 100\% \tag{2}$$

$$U = \frac{\text{(area of change during all intervals)/(area of study region)}}{\text{duration of all intervals}} \times 100\% = \frac{\sum_{t=1}^{T-1} \left\{ \sum_{j=1}^{J} \left[\left(\sum_{i=1}^{J} C_{tij} \right) - C_{tij} \right] \right\} / \left[\sum_{j=1}^{J} \left(\sum_{i=1}^{J} C_{tij} \right) \right]}{[Y_T - Y_1]} \times 100\% \tag{3}$$

$$
\begin{aligned}
\mathrm{G}_{\mathrm{tj}} &= \frac{\left(\text{area of gross gain of category j during}[\mathrm{Y}_{\mathrm{t}}, \mathrm{Y}_{\mathrm{t+1}}]\right)/(\text{duration of}[\mathrm{Y}_{\mathrm{t}}, \mathrm{Y}_{\mathrm{t+1}}])}{\text{area of category j at time } \mathrm{Y}_{\mathrm{t+1}}} \times 100\% \\
&= \frac{\left[\left(\sum_{i=1}^{J} C_{tij}\right) - C_{tjj}\right]/\left(\mathrm{Y}_{\mathrm{t+1}} - \mathrm{Y}_{\mathrm{t}}\right)}{\sum_{i=1}^{J} C_{tij}} \times 100\%
\end{aligned}
\tag{4}
$$

$$
\begin{aligned}
\mathrm{L}_{\mathrm{ti}} &= \frac{\left(\text{area of gross loss of categor y i during}[\mathrm{Y}_{\mathrm{t}}, \mathrm{Y}_{\mathrm{t+1}}]\right)/(\text{duration of}[\mathrm{Y}_{\mathrm{t}}, \mathrm{Y}_{\mathrm{t+1}}])}{\text{area of category i at time } \mathrm{Y}_{\mathrm{t}}} \times 100\% \\
&= \frac{\left[\left(\sum_{j=1}^{J} C_{tij}\right) - C_{tii}\right]/\left(\mathrm{Y}_{\mathrm{t+1}} - \mathrm{Y}_{\mathrm{t}}\right)}{\sum_{j=1}^{J} C_{tij}} \times 100\%
\end{aligned}
\tag{5}
$$

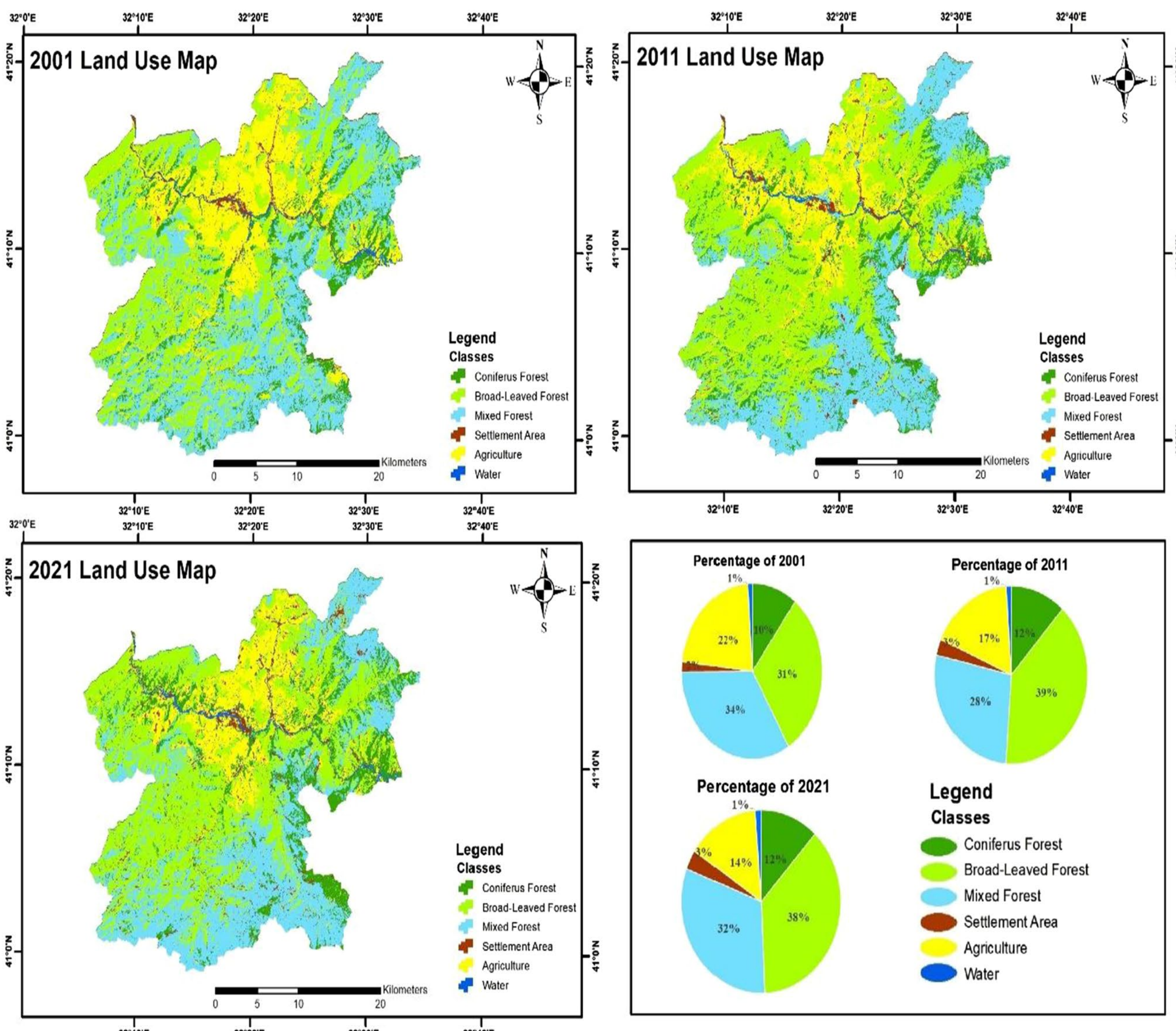

Fig. 4 Time series of land use and cover maps (2001, 2011 and 2021) of Landsat ETM + and OLI-controlled classified images of the study area

The pass level compares how each category earns from other categories in each time interval (Quan et al 2020; Ekumah 2020). This level of intensity analysis analyzes based on the results from Eq. 5 and 6 whether the gains of one category are heavily targeting the losses of the other categories at the start of each time interval. Equation gives the annual transition density (Rtin) observed from category i to category n during the time interval (Yt, Yt + 1) according to the dimension (Yt) at the beginning of the time interval of category i. Equation gives the annual uniform transition density (Wtn), which represents the situation when category n is assumed to gain uniformly across the entire landscape in the time interval (Yt, Yt + 1). According to the results of the analysis, when Rtin > Wtn, category i's losses are targeted as gains by category n in the t time interval, and when Rtin < Wtn, category n avoids targeting category i losses as gains (Kaptan 2021).

Table 3 Accuracy and error matrix values of Ladsat ETM + and OLI-controlled classified images (1999, 2009 and 2019)

2001	Coniferous Forest	Broad-Leaved Forest	Mixed Forest	SettlementArea	Agriculture	Water	Total	User´s accuracy (%)
Coniferous forest	8898	459	1470	0	1340	35	12,202	72.92
Broad-leaved Forest	16	48,251	1266	0	1148	0	50,681	95.21
Mixed forest	464	4675	23,255	0	136	0	28,530	81.51
Settlement area	56	2	15	2232	1339	302	3946	56.56
Agriculture	301	2105	138	724	46,297	100	49,665	93.22
Water	279	2	0	177	491	2147	3096	69.35
Total	10,014	55,494	26,144	3133	50,751	2584	148,120	–
Producer´s accuracy (%)	88.86	86.95	88.95	71.24	91.22	83.09	–	–
Overall accuracy = 88.495% Kappa coefficient: 0.83								
2011	Coniferous forest	Broad-Leaved Forest	Mixed Forest	SettlementArea	Agriculture	Water	Total	User´s accuracy (%)
Coniferous forest	7602	544	2763	25	332	88	11,354	66.95
Broad-leaved forest	348	44,104	1559	22	1328	73	47,434	92.98
Mixed forest	284	498	49,257	159	15	39	50,252	98.02
Settlement area	56	125	1672	5222	775	623	8473	61.63
Agriculture	303	1240	63	476	25,162	271	27,515	91.45
Water	13	24	8	369	34	3168	3616	87.61
Total	8606	46,535	55,322	6273	27,646	4262	148,644	–
Producer´s accuracy (%)	88.33	94.78	89.04	83.25	91.01	74.33	–	–
Overall accuracy = 90.494% Kappa coefficient: 0.87								
2021	Coniferous Forest	Broad-Leaved Forest	Mixed Forest	SettlementArea	Agriculture	Water	Total	User´s accuracy (%)
Coniferous Forest	10,177	831	1088	34	441	149	12,720	80.01
Broad-Leaved Forest	1067	51,897	3670	7	2319	35	58,995	87.97
Mixed Forest	795	2174	56,433	15	98	2	59,517	94.82
Settlement Area	215	646	1057	2454	906	356	5634	43.56
Agriculture	402	838	94	189	34,668	470	36,661	94.56
Water	283	3	0	185	248	3294	4013	82.08
Total	12,939	56,389	62,342	2884	38,680	4306	177,540	–
Producer´s accuracy (%)	78.65	92.03	90.52	85.09	89.63	76.50	–	–
Overall accuracy = 89.513% Kappa coefficient: 0.85								

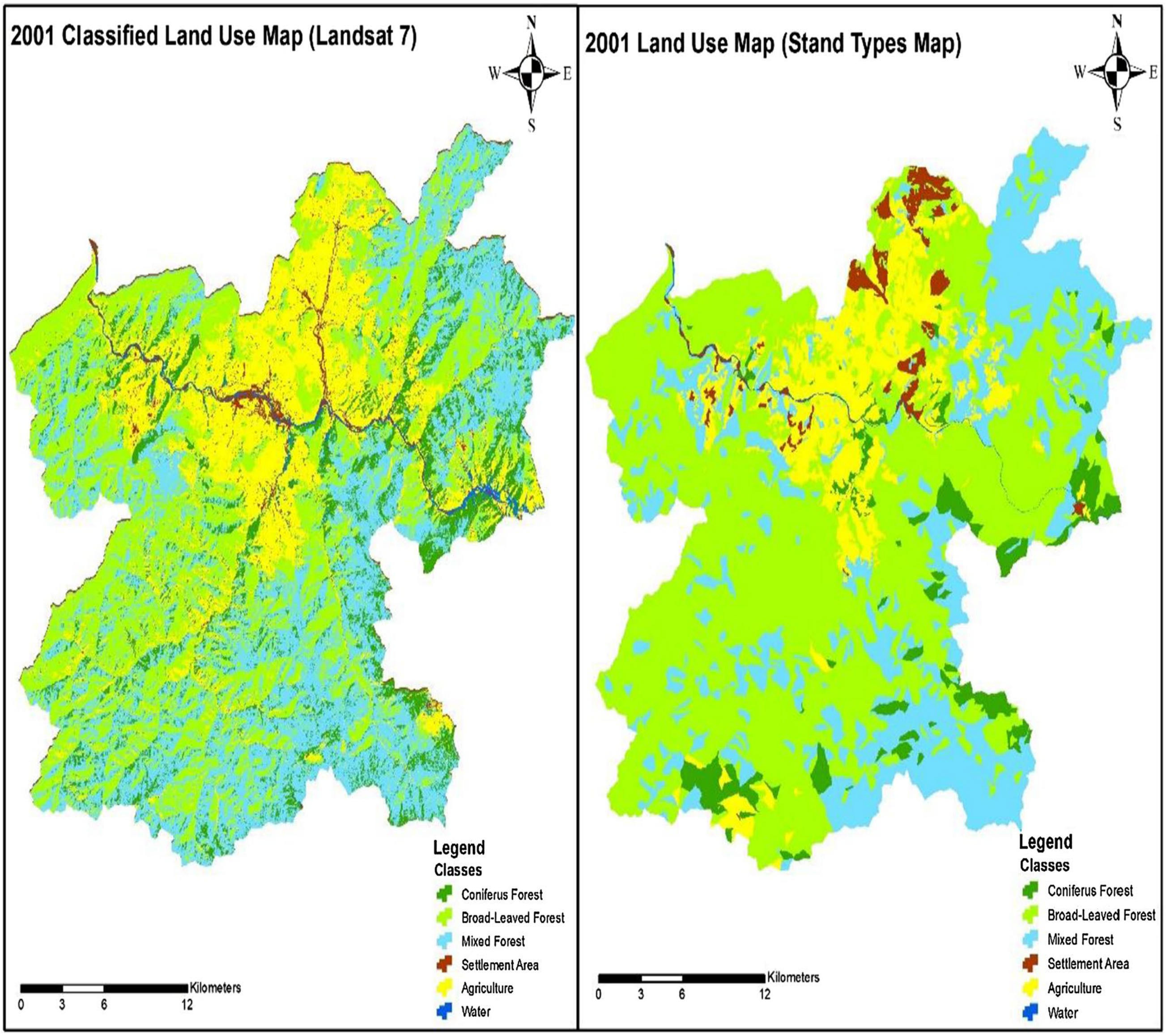

Fig. 5 Land use maps of 2001 classified Landsat and stand types map

$$
\begin{aligned}
\mathrm{R_{tin}} &= \frac{\left(\text{area of transition from i to n during } [\mathrm{Y_t}, \mathrm{Y_{t+1}}]\right)/(\text{duration of } [\mathrm{Y_t}, \mathrm{Y_{t+1}}])}{\text{area of category i at time } \mathrm{Y_t}} \times 100\% \\
&= \frac{C_{tin}/\left(\mathrm{Y_{t+1}} - \mathrm{Y_t}\right)}{\sum_{j=1}^{J} C_{tij}} \times 100\% \\
\mathrm{W_{tn}} &= \frac{\left(\text{area of gross gain of category n during } [\mathrm{Y_t}, \mathrm{Y_{t+1}}]\right)/(\text{duration of } [\mathrm{Y_t}, \mathrm{Y_{t+1}}])}{\text{area of category n at time } \mathrm{Y_t}} \times 100\% \\
&= \frac{\left[\left(\sum_{i=1}^{J} C_{tin}\right) - C_{tin}\right]/\left(\mathrm{Y_{t+1}} - \mathrm{Y_t}\right)}{\sum_{i=1}^{J}\left[\left(\sum_{i=1}^{J} C_{tij}\right) - C_{tnj}\right]} \times 100\%
\end{aligned}
\tag{6}
$$

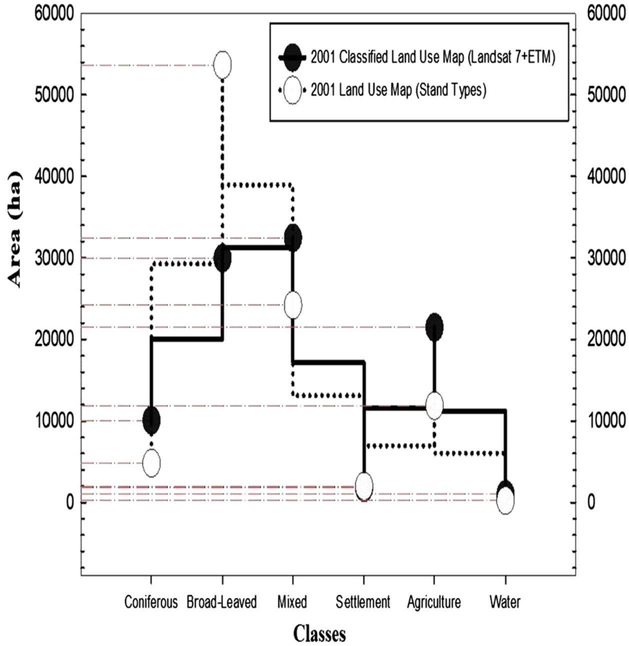

Fig. 6 Land use maps of the year 2001 classified Landsat and stand types map

Results and discussion

Results

Supervised classification and accuracy assessment

Classification for coniferous forest, mixed forest, broad-leaved forest, settlement, agriculture and water, which consists of 6 categories, land use maps for the years 2001, 2011 and 2021 were classified as controlled by reference to the stand types maps of the relevant years (Fig. 4). The accuracy indices and error matrix values of the land use maps obtained as a result of the classification were calculated (Table 3). When Table 3 is examined, it is seen that the control pixel numbers of the classes and the area (ha) values are directly proportional. It is seen that the water class, which represents the smallest area in the study area in all three periods in terms of reference pixel number, was used in the 2001 classification with the minimum reference pixel number of 3096 pixels among the classes.

The overall accuracy for the 2001 land use map is 88.495% and the kappa coefficient is 0.83, which indicates that the accuracy of the controlled classification is statistically high and the ability to represent the study area is high.

Table 4 LULC area values for the period 2001–2011 and 2011–2021

2001	2011									
	Coniferous	Broad-Leaved	Mixed	Settlement	Agriculture	Water	Total	Gain	Loss	Net Change
Coniferous	5,608.9	1,714,5	1,865.1	48.8	803.8	49.7	10,090.6	5,728.2	4,481.8	1,246.4
Broad-leaved	106.4	22,828,6	4,555.4	358.2	2,089.8	14.3	29,952.8	15,352.8	7,124.1	8,228.7
Mixed	4,435.3	8,686,9	18,479.7	302.8	519.3	26	32,450	8,088.6	13,970.2	−5,881.6
Settlement	10.3	26.9	455.1	781.8	319.2	225.9	1,819.2	2,051.2	1.037.4	1,013.8
Agriculture	864.5	4,898.4	1.53.4	1,216.4	12,981	353.2	21,467	3,856.9	8,486.0	−4,629.1
Water	311.7	26.2	59.6	125	124.9	376.3	1,023.6	669.1	647.3	21,8
Total	11,337.1	38,181.5	26,568.3	2,833.1	16,837.9	1,045.4	96,803.2			

2011	2021									
	Coniferous	Broad-Leaved	Mixed	Settlement	Agriculture	Water	Total	Gain	Kayıp	Net Change
Coniferous	5,560.5	615.4	4,835	84.3	163.5	78.2	11,336.8	5,850.4	5,776.2	74.2
Broad-Leaved	1,517.7	28,276.6	5,339.8	366.6	2.65	28	38,180.7	8,040.3	9,904.1	−1,863.8
Mixed	2,607.6	3,143.8	19,597.7	848.7	290.3	83.5	26,571.5	10,932.4	6,973.9	3,958.5
Settlement	441.4	300.4	325.7	993.4	510.6	259.3	2,830.9	2,352	1,837.4	514.6
Agriculture	1,191.1	3,955.8	406,9	863.4	10,179.4	241.3	16,837.9	3,782.8	6,658.5	−2,875.7
Water	92.7	24.9	25	189.1	166.5	547.2	1,045.4	690.4	498.2	192.2
Total	11,411	36,317	30,530	3,345.5	13,962.2	1,237.6	96,803.2			

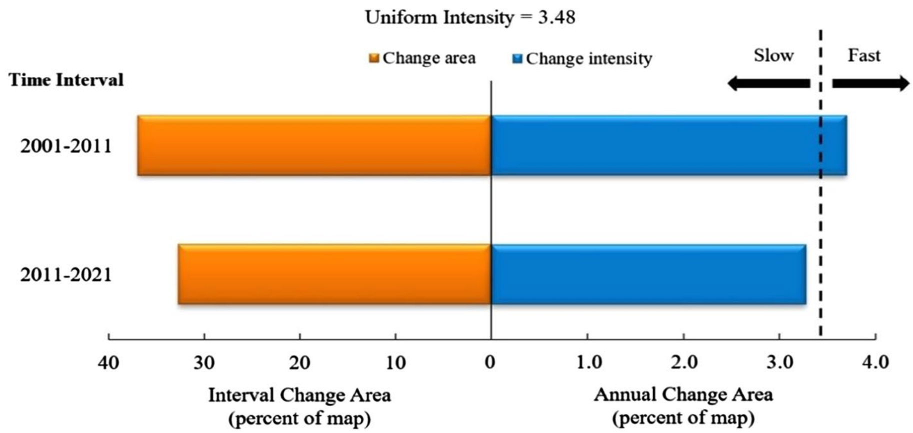

Fig. 7 Interval level density analysis for the 1993–2004 and 2004–2015 time periods

For the thematic map of 2001, highest Producer´s accuracy values (≥ 80%), respectively, it belongs to agriculture, mixed forest, coniferous forest, broad-leaved forest and water classes. The lowest Producer´s accuracy belongs to the settlement area class with 71.24%. It was concluded that the highest value of User´s accuracy was in broad-leaved forest (95.21%) and agriculture (56.56%) while the class with the lowest value (Table 3). The land use maps of 2001 stand types and classified satellite imagery are shown in Fig. 5, and the areal values of these maps are shown in Fig. 6.

When the classification results of 2011 are examined, overall accuracy (overall accuracy) was 90.494% and Kappa coefficient was 0.87. All classes are above 85% except for the Producer´s accuracy water (74.33%) class. It belongs to the broad-leaved class with the highest manufacturer accuracy of 94.78%. User´s accuracy (%) rates are; Coniferous forest 66.95%, broad-leaved forest 92.98%, mixed forest 98.02%, settlement area 61.63%, agriculture 91.45% and water 87.61%, the highest user accuracy belongs to broad-leaved class.

When the classification accuracy values of 2021 were examined, the overall accuracy rate was calculated as 89.513% and the Kappa coefficient as 0.85. Producer accuracy rates for the land use map of 2021 for each class; coniferous forest 78.65%, broad-leaved forest 92.03%, mixed forest 90.52%, settlement area 85.09%, agriculture 89.63% and water 76.50%. User´s accuracy (%) rates are over 80% in all classes except settlement area (43.56%) and the highest User´s accuracy value belongs to mixed forest class with 94.82%.

Changes in LULC in the study area

The land transition matrix showing the LULC changes in the study area between 2001–2011 and 2011–2021 is given in Table 4. According to the table, the category with the widest distribution in 2001, 2011 and 2021 is the Broad-Leaved and Mixed category. These two categories are followed by Agriculture, Coniferous, Settlement and Water categories, respectively, according to the area size.

According to the findings obtained from the study, it was determined that from 2001 to 2021, there was an increase of approximately 8% in forest area and a decrease of 24% in non–forest areas. While the mixed forest decreased by 18% in the first time period covering 2001–2011, it experienced an increase of 12% in the 2011–2021 time period. Broad-Leaved, on the other hand, increased by 27% in the first timeframe and decreased by 6% in the second timeframe. Coniferous increased by 12% and 1%, respectively, in both time intervals. At the end of the 20-year period from 2001 to 2021, Coniferous and Broad-Leaved grew by 13% and 21%, respectively, while the Mixed forest shrank by 6%.

In the non-forest area class, in the 20-year period from 2001 to 2021, Settlement and Water increased by 84% and 21%, respectively, while Agriculture decreased by 35%. In the period 2001–2011 Settlement expanded by 56% and Water by 2%, while Agriculture contracted by 22%. In the period of 2011–2021, the situation did not change much, while Settlement increased by 28%, Water increased by 19%, while Agriculture decreased by 13%.

Intensity analysis

Interval level

According to the land use change matrix (land use change matrix) for the 2001–2011 and 2011–2021 time periods, the total amount of land-use change in each period, annual change intensity and the intensity of change is shown in Fig. 7.

Each bar on the left side of the central axis of the graph indicates the percent of change level experienced in time intervals, and the bars on the right indicate the intensity of the changes observed. The fact that the bar for the period 2001–2011 on the right (annual change rate 3.69%) extends beyond the uniform line indicates that the land use change is

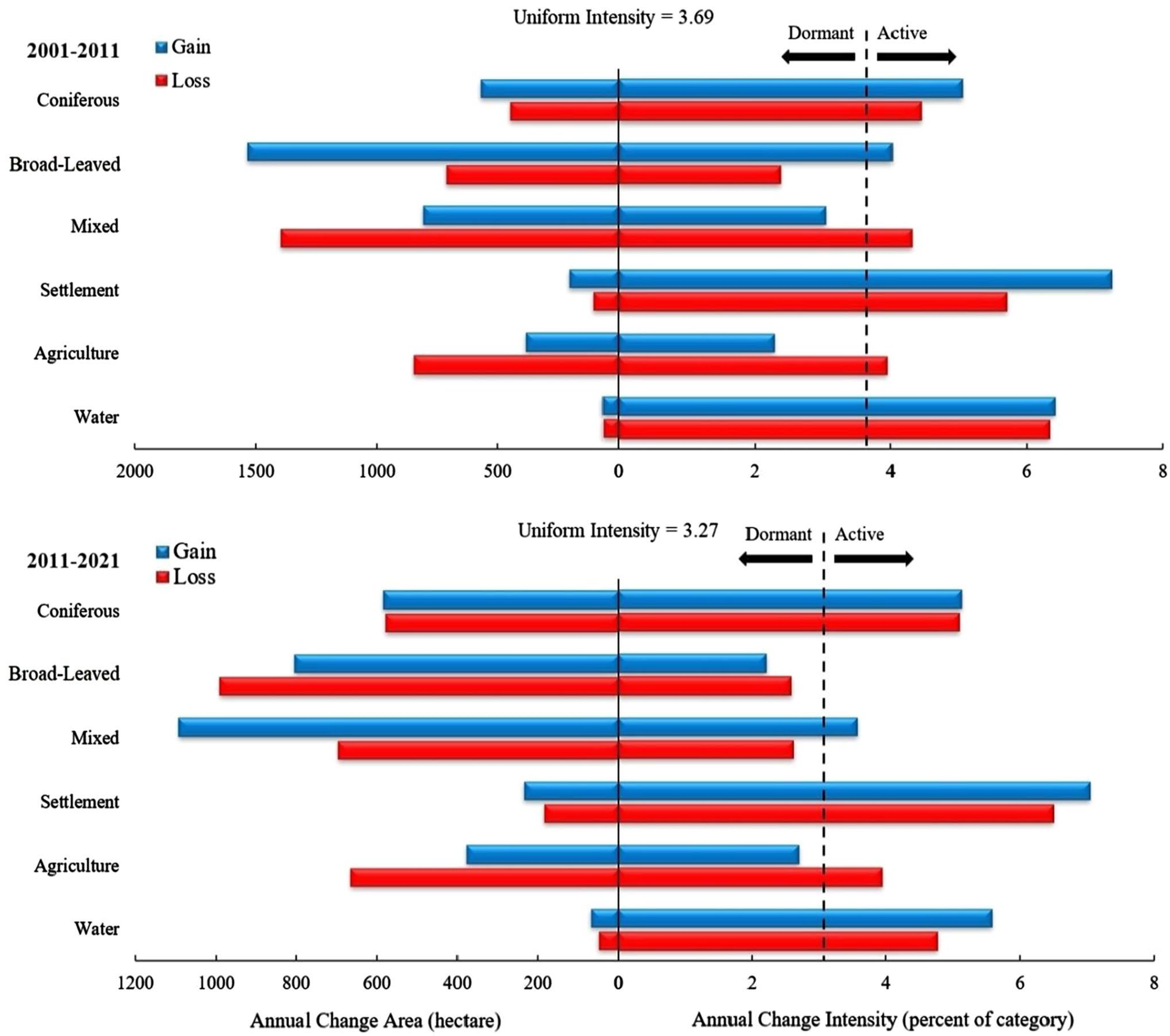

Fig. 8 Time intensity analysis for two time intervals: 2001–2011 and 2011–2021

rapid in this period, while the bar for the period 2011–2021 (annual change rate 3.27%) is finished before reaching the uniform line means that land use change is slow during this period. If annual changes in categories were constant over the entire temporal range, both bars extending to the right would be above the uniform line.

Category level

Figure 8, showing the results of the density analysis for the category level, shows the annual area changes and annual variation intensities in terms of gross loss and gross gain in each category at each time interval.

While Broad-Leaved was the category with the biggest gains in the first time slot, it was the category with the biggest loss in the second time slot. While Mixed was the category with the biggest loss in the first time slot, it was the category with the biggest gain in the second time slot. While the coniferous category is higher than its gain in the first time slot, its loss and gain in the second time slot are almost equal. While Agriculture continues to experience losses in both time periods, the gain is greater than the loss for the Settlement and Water category.

To better understand the transitions between categories, it is necessary to look at the annual density changes on the right side of the graph showing the results of the density analysis. According to this, in the first time period, all

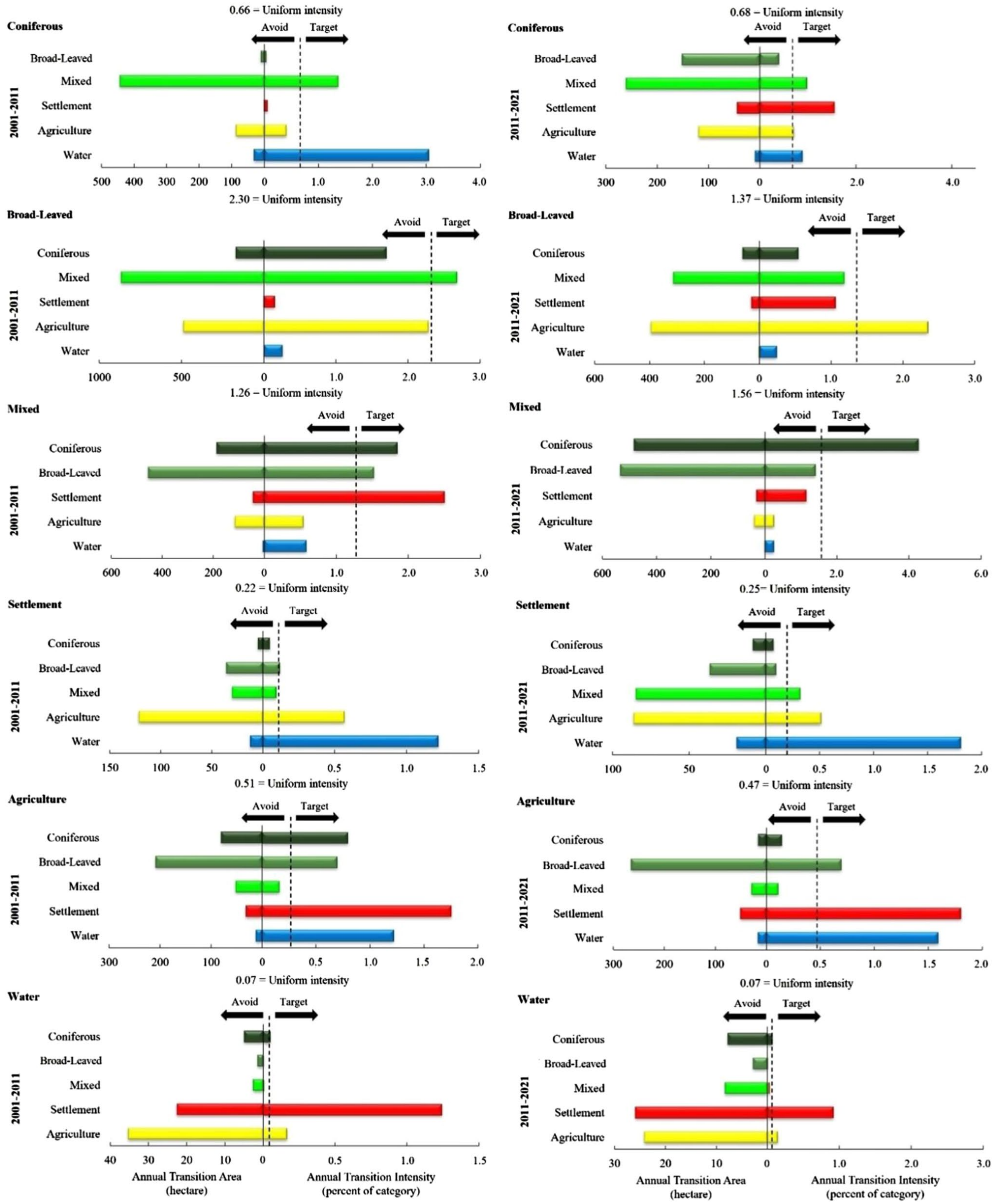

Fig. 9 Transition intensity analysis for the gains of categories during the two-time intervals

categories except Broad-Leaved and Agriculture are active in terms of both loss and gain. Broad-Leaved is an active winner in the first time slot, while dormant in both loss and gain in the second time slot. Mixed is active in terms of losses in the first time slot and active winner in the second time slot. Coniferous, Settlement and Water categories are active in both timeframes in terms of loss and gain. The gain of the Coniferous category in the first time slot is greater than its loss, while it is almost equal in the second time slot. Agriculture, on the other hand, is an active loser in both time periods. The gain of the Water category is more active than the loss in both time intervals.

Transition level

In Fig. 9, which shows the results of the transition level analysis, the left side of each graph gives the size of the annual transitions and the right side gives the intensity of the annual transitions. Aiming Mixed and Water losses as gains in the 2001–2011 timeframe, Coniferous also targeted Settlement losses as gains in the 2011–2021 timeframe along with these categories. The gain of Broad-Leaved heavily targeted Mixed losses in the first timeframe and Agriculture losses in the second timeframe. Mixed heavily targeted Coniferous, Borad-Leaved and Settlement losses as gains in the first timeframe, while heavily targeting only Coniferous losses in the second timeframe.

While the gain of Settlement targeted Agriculture and Water losses in the first timeframe, it also targeted Mixed losses as gains in the second timeframe. Agriculture targeted losses of all categories except Mixed in the first timeframe, while avoiding targeting Coniferous losses with Mixed in the second timeframe (avoid). Agriculture targeted Settlement losses most intensely in both time periods. The Water category targeted Settlement and Agriculture losses as gains in both time periods.

Discussion

The use of Landsat 7 ETM + and Landsat 8 OLI/TIRS from Landsat satellite images, which can include Multispectral Scanner (MSS), Enhanced Thematic Mapper Plus (ETM +), Thematic Mapper (TM), and Operational Land Imager (OLI), is effective in improving LULC classification accuracy. Apan (1997), Tole (2002), and Reis (2008) searched that MSS classification results were given lower classification accuracy for LULC. Pang et al. (2013) in the analysis of 1979 (MSS), 1992 (TM), 2001 (ETM +) and 2006 (TM) Landsat satellite images and examining deforestation and consequent land use change patterns, it was emphasized that the 1979 Landsat MSS image is more difficult to classify than other Landsat images. Doaemo et al. (2020) stated in their preliminary study that they encountered problems caused by cloud cover (like the cultivated areas may be mixed with bare areas after harvest). They stated that they intend to solve these problems by using LULC classification systems such as forest land, barren, wetland, water, agriculture and settlement, which are very similar to the classification applied by us in future studies. Therefore, with such a classification, they aim to better evaluate the LULC activities taking place in their study areas. Also, Clerici et al. (2017), Reiche et al. (2018) and Wang et al. (2019) in order to eliminate the gaps caused by the low resolution of Landsat sensors; 10 m resolution open source images presented by Sentinel sensors can be examined in shorter time intervals and the most suitable periods can be selected for evaluations.

It has been proven that semi-autonomous observation of forest areas is possible with Unmanned Aerial Vehicles (UAV) and LIDAR, with the developments in image processing techniques and the increase in the use of machine learning algorithms (Tan and Shao 2015; Mohan et al. 2017; Almeida et al. 2019). However, the unsuitable cost of UAV and LIDAR for large areas and systematic repeated measurements shows that satellite imagery is still the most suitable option for large-scale studies.

While conducting the LULC analysis, forest areas have increased by approximately 8% in Yenice Forest Operation Directorate, despite focusing on the reduction in forest areas that will occur in most studies at all time intervals considered. The maximum change occurred between 2001 and 2011. As of 2001, less effort has been spent for the Yenice Forest Operation Directorate, which consists of forest areas with a high rate of approximately 82.5% compared to the studies to determine the spatial forest area changes in Turkey. According to the management plans repeated over the years, the study area had 87.9% forest cover in 1985, 82.5% in 2001, followed by 84.8% and 87% in 2011 and 2021, respectively. In many studies focusing on the shrinkage of forest areas (Ningal et al. 2008; Mohajena et al. 2018; Doaemo et al. 2020), agriculture is among the reasons for the 50% decrease in forest area per capita. is shown. For the study area, it can be said that this situation works on the contrary with its emigrant structure. The population, which was 26,951 as of 2000, decreased by approximately 25% in 2020 to 20,116. According to TUIK data, the annual population growth of Yenice is −9.6% (TUIK 2021). Therefore, both the decrease in the population and the fact that a large part of the study area is covered with forests, reduce the negative social pressure on the area.

From the analyses of the LULC changes, the fact that there has not been a major change in the total forest cover despite the global climate change, which is accepted by all, may be the result of the great efforts of the forestry organization (1375 ha afforestation and 2668 ha rehabilitation and artificial regeneration works carried out since 2001).

In addition, the fact that it has a Nature Conservation Area (within Kavaklı and Çitdere Forest Sub-district directorate) covering approximately 1.4% of the study area since 1987 (Şahin 2021) is thought to have contributed to the low change in forest areas, albeit partially. The methodology applied in this study may be useful in planning the use of forest resources and in developing strategies to make the existence of the examined forest sustainable.

Conclusion

In this study, the changes in forest areas and land cover of Yenice region of Turkey between 2001 and 2021 were examined by density analysis using GIS and remote sensing techniques at three levels, namely interval level, category level and transition level. While there was an increase in the total forest area during the study period, a decrease was detected in the non-forest area. Interval level results of the density analysis showed that the rate of change of land use in the period 2001–2011 was faster than in the period 2011–2021. It is seen that the increase in forest area in the period of 2001 and 2021 is over 800 m in the southern parts of the operation directorate, and the decrease in non-forest areas is concentrated in the western parts. In future studies, processing data from high resolution images via LIDAR or Unmanned Aerial Vehicles (UAV) instead of Landsat satellite images will help gather more information on behalf of these communities in order to learn more about tree populations in various developmental ages. At the same time, such data could be a valuable complement to optical data from satellites. Regardless of the data collection method, we can agree that the changes due to global climate change should be examined in the evaluation of LULC and taken into account in the development and implementation of managerial practices. Rapidly occurring and successive changes, such as drought, large fires and insect damage, may not be monitored over 10-year periods from time to time. To eliminate this handicap, Landsat data can detect precise changes that occur each year. At the same time, accurate annual information about the change in forest areas and the regeneration of forests can provide practitioners with different perspectives. It is still not clear whether the increase in forest areas is the result of OGM's (General Directorate of Forestry) success in afforestation efforts to protect degraded areas or the result of rural–urban migration, which is a reality of Turkey. When this situation is clarified, it will shed light on what managers should focus on in order to protect and develop forested areas. As in our study, we think that the change studies in forest areas, which will be carried out on a small scale in general, will help decision makers in the implementation of preventive measures as well as providing more detailed information. In the first 10-year period (2001–2011), residential areas in the region, and in the second 10-year period (2011–2021), area gain from mixed stands necessitates the determination of the course of urban development, which annual change data will also allow.

Acknowledgements The authors thank the supported by the Republic of Turkey Ministry of Agriculture and Forestry, General Directorate of Forest Engineering and the General Directorate of Meteorology for their prompt responses to our requests.

Author contributions HA, SK, TV, MC, HBO designed the study and performed the experiments; HA, SK, TV, HBO and MC performed the experiments, analyzed the data, and wrote the manuscript.

Funding Not applicable.

Availability of data and materials Not applicable.

Declarations

Conflict of interest Not applicable. Authors declare no conflict of interest.

Human and animals participants This article does not contain any studies with human participants or animals performed by any of the authors.

References

Abd El-Kawy OR, Rød JK, Ismail HA, Suliman AS (2011) Land use and land cover change detection in the western Nile delta of Egypt using remote sensing data. Appl Geogr 31(2):483–494. https://doi.org/10.1016/j.apgeog.2010.10.012

Acheampong M, Yu Q, Enomah LD, Anchang J, Eduful M (2018) Land use/cover change in Ghana's oil city: assessing the impact of neoliberal economic policies and implications for sustainable development goal number one–a remote sensing and GIS approach. Land Use Policy 73:373–384. https://doi.org/10.1016/j.landusepol.2018.02.019

Akinyemi FO, Pontius RG Jr, Braimoh AK (2017) Land change dynamics: insights from intensity analysis applied to an African emerging city. J Spat Sci 62(1):69–83. https://doi.org/10.1080/14498596.2016.1196624

Aksoy H, Kaptan S (2020) Simulation of future forest and land use/cover changes (2019–2039) using the cellular automata-Markov model. Geocarto Int. https://doi.org/10.1080/10106049.2020.1778102

Aldwaik SZ, Pontius RG Jr (2012) Intensity analysis to unify measurements of size and stationarity of land changes by interval, category, and transition. Landsc and Urban Plan 106(1):103–114. https://doi.org/10.1080/14498596.2016.1196624

Aldwaik SZ, Pontius RG Jr (2013) Map errors that could account for deviations from a uniform intensity of land change. Int J Geogr Inf Syst 27(9):1717–1739. https://doi.org/10.1080/13658816.2013.787618

Almeida DRA, Broadbent EN, Zambrano AMA, Wilkinson BE, Ferreira ME, Chazdon R, Meli P, Gorgens EB, Silva CA, Stark SC, Valbuena R, Papa DA, Brancalion PHS (2019) Monitoring the structure of forest restoration plantations with a drone-lidar system. Int J Appl Earth Obs Geoinf 79: 192–198. https://www.sciencedirect.com/science/article/abs/pii/S0303243418311954

Apan AA (1997) Land cover mapping for tropical forest rehabilitation planning using remotely-sensed data. Int J Remote Sens 18(5): 1029–1049. https://www.tandfonline.com/doi/abs/https://doi.org/10.1080/014311697218557

Barakat A, Ouargaf Z, Khellouk R, El Jazouli A, Touhami F (2019) Land use/land cover change and environmental impact assessment in béni-mellal district (morocco) using remote sensing and GIS. Earth Sys Environ 3(1):113–125. https://doi.org/10.1007/s41748-019-00088-y

Berakhi RO, Oyana TJ, Adu-Prah S (2015) Land use and land cover change and its implications in Kagera river basin. East Africa Afr Geogr Rev 34(3):209–231. https://doi.org/10.1080/19376812.2014.912140

Bozali N, Sivrikaya F, Akay AE (2015) Use of spatial pattern analysis to assess forest cover changes in the Mediterranean region of Turkey. J for Res 20(4):365–374. https://doi.org/10.1007/s10310-015-0493-2

Clerici N, Valbuena Calderón CA, Posada JM (2017) Fusion of Sentinel-1A and Sentinel-2A data for land cover mapping: a case study in the lower Magdalena region, Colombia. J Maps 13(2): 718–726. https://www.tandfonline.com/doi/full/https://doi.org/10.1080/17445647.2017.1372316

Çoban H, Gündoğdu Ş (2020) GIS-based determination of changes in forest areas: the example of Çamsu Forestry operations directorate. Turk J for 21(1):60–69. https://doi.org/10.18182/tjf.693465

Doaemo W, Mohan M, Adrah E, Srinivasan S, Dalla Corte AP (2020) Exploring Forest Change Spatial Patterns in Papua New Guinea: A Pilot Study in the Bumbu River Basin. Land 9(9): 282. https://www.mdpi.com/2073-445X/9/9/282

Duan H, Xie Y, Du T, Wang X (2021) Random and systematic change analysis in land use change at the category level–a case study on Mu Us area of China. Sci Total Environ 777:145920. https://doi.org/10.1016/j.scitotenv.2021.145920

Ekumah B, Armah FA, Afrifa EK, Aheto DW, Odoi JO, Afitiri AR (2020) Assessing land use and land cover change in coastal urban wetlands of international importance in Ghana using intensity analysis. Wetl Ecol Manag 28:1–14. https://doi.org/10.1007/s11273-020-09712-5

FAO (2020) Food and Agriculture Organization of the United Nations. Global Forest Resources Assessment 2020 – Key findings Rome https://doi.org/10.4060/ca8753enaccessedon05.04.2021

Foley JA, DeFries R, Asner GP, Barford C, Bonan G, Carpenter SR, Chapin FS, Coe MT, Daily GC, Gibbs JH, Helkowski JH, Holloway EA, Kucharik CJ, Monfreda C, Patz JA, Prentice IC, Ramankutty N, Snyder PK (2005) Global consequences of land use. Science 309(5734):570–574. https://doi.org/10.1126/science.1111772

Friedl MA, Brodley CE, Strahler AH (1999) Maximizing land cover classification accuracies produced by decision trees at continental to global scales. IEEE Trans Geosci Remote Sens 37(2): 969–977. https://ieeexplore.ieee.org/abstract/document/752215/

Gadrani L, Lominadze G, Tsitsagi M (2018) F assessment of landuse/landcover (LULC) change of Tbilisi and surrounding area using remote sensing (RS) and GIS. Ann Agrar Sci 16(2):163–169. https://doi.org/10.1016/j.aasci.2018.02.005

Guo M, Ma S, Wang LJ, Lin C (2021) Impacts of future climate change and different management scenarios on water-related ecosystem services: a case study in the Jianghuai ecological economic Zone. China Ecol Indic 127:107732. https://doi.org/10.1016/j.ecolind.2021.107732

Halmy MWA, Gessler PE, Hicke JA, Salem BB (2015) Land use/land cover change detection and prediction in the north-western coastal desert of Egypt using Markov-CA. Appl Geogr 63:101–112. https://doi.org/10.1016/j.apgeog.2015.06.015

Han Z, Song W, Deng X (2016) Responses of ecosystem service to land use change in Qinghai Province. Energies 9(4):303. https://doi.org/10.3390/en9040303

Hassan Z, Shabbir R, Ahmad SS, Malik AH, Aziz N, Butt A, Erum S (2016) Dynamics of land use and land cover change (LULCC) using geospatial techniques: a case study of Islamabad Pakistan. Springerplus 5(1):1–11. https://doi.org/10.1186/s40064-016-2414-z

Huang J, Pontius RG Jr, Li Q, Zhang Y (2012) Use of intensity analysis to link patterns with processes of land change from 1986 to 2007 in a coastal watershed of southeast China. Appl Geogr 34:371–384. https://doi.org/10.1016/j.apgeog.2012.01.001

Huang B, Huang J, Pontius RG Jr, Tu Z (2018) Comparison of Intensity Analysis and the land use dynamic degrees to measure land changes outside versus inside the coastal zone of Longhai, China. Ecol Indic 89:336–347. https://doi.org/10.1016/j.ecolind.2017.12.057

Kaptan S, Durkaya A (2019) Analysing temporal and spatial changes in land cover: the case of Drahna Forest Subdistrict directorate. Kastamonu Uni J for Fac 191:47–56. https://doi.org/10.17475/kastorman.543428

Kaptan S (2021) Changes in forest areas and land cover and their causes using intensity analysis: the case of Alabarda Forest Planning Unit. Environ Monit Assess (accepted but not yet published).

Kindu M, Schneider T, Teketay D, Knoke T (2015) Drivers of land use/land cover changes in Munessa-Shashemene landscape of the south-central highlands of Ethiopia. Environ Monit Assess 187(7):452. https://doi.org/10.1007/s10661-015-4671-7

Kourosh Niya A, Huang J, Karimi H, Keshtkar H, Naimi B (2019) Use of intensity analysis to characterize land use/cover change in the biggest island of Persian Gulf, Qeshm Island. Iran Sustain 11(16):4396. https://doi.org/10.3390/su11164396

Manakos I, Braun M (2014) Land use and land cover mapping in Europe. Springer, London 18:411

Manandhar R, Odeh IO, Pontius RG Jr (2010) Analysis of twenty years of categorical land transitions in the Lower Hunter of New South Wales. Australia Agri Ecosyst Environ 135(4):336–346. https://doi.org/10.1016/j.agee.2009.10.016

Mohajane M, Essahlaoui A, Oudija F, Hafyani ME, Hmaidi AE, Ouali AE, Randazzo G, Teodoro AC (2018) Land use/land cover (LULC) using landsat data series (MSS, TM, ETM+ and OLI) in Azrou Forest, in the Central Middle Atlas of Morocco. Environments 5(12): 131. https://www.mdpi.com/2076-3298/5/12/131

Mohan M, Silva CA, Klauberg C, Jat P, Catts G, Cardil A, Hudak AT, Dia M (2017) Individual tree detection from unmanned aerial vehicle (UAV) derived canopy height model in an open canopy mixed conifer forest. Forests 8(9): 340. https://www.mdpi.com/1999-4907/8/9/340

Niemelä J, Kotze J, Ashworth A, Brandmayr P, Desender K, New T, Penev L, Samways M, Spence J (2000) The search for common anthropogenic impacts on biodiversity: a global network. J Insect Conserv 4(1):3–9. https://doi.org/10.1023/A:1009655127440

Ningal T, Hartemink AE, Bregt AK (2008) Land use change and population growth in the Morobe Province of Papua New Guinea between 1975 and 2000. J Environ Manage 87(1): 117–124. https://www.sciencedirect.com/science/article/pii/S0301479707000266

Nyamekye C, Kwofie S, Ghansah B, Agyapong E, Boamah LA (2020) Assessing urban growth in Ghana using machine learning and intensity analysis: a case study of the new Juaben Municipality. Land Use Policy 99:105057. https://doi.org/10.1016/j.landusepol.2020.105057

OGM (2021) TR Ministry of Agriculture and Forestry, General Directorate of Forestry (OGM), https://www.ogm.gov.tr/tr [accessed on 14/05/2021]

Pang C, Yu H, He J, Xu J (2013) Deforestation and changes in landscape patterns from 1979 to 2006 in Suan County, DPR Korea. Forests 4(4): 968–983. https://www.mdpi.com/1999-4907/4/4/968

Paul S, Saxena KG, Nagendra H, Lele N (2021) Tracing land use and land cover change in peri-urban Delhi, India, over 1973–2017 period. Environ Monit Assess 193(2):1–12. https://doi.org/10.1007/s10661-020-08841-x

Peng J, Liu Y, Wu J, Lv H, Hu X (2015) Linking ecosystem services and landscape patterns to assess urban ecosystem health: a case study in Shenzhen City, China. Landsc Urban Plan 143:56–68. https://doi.org/10.1016/j.landurbplan.2015.06.007

Pontius RG Jr, Shusas E, McEachern M (2004) Detecting important categorical land changes while accounting for persistence. Agric Ecosyst Environ 101(2–3):251–268. https://doi.org/10.1016/j.agee.2003.09.008

Quan B, Pontius RG Jr, Song H (2020) Intensity Analysis to communicate land change during three time intervals in two regions of Quanzhou City. China Gisci Remote Sens 57(1):21–36. https://doi.org/10.1080/15481603.2019.1658420

Reiche J, Hamunyela E, Verbesselt J, Hoekman D, Herold M (2018) Improving near-real time deforestation monitoring in tropical dry forests by combining dense Sentinel-1 time series with Landsat and ALOS-2 PALSAR-2. Remote Sens Environ 204: 147–161. https://www.sciencedirect.com/science/article/abs/pii/S0034425717304959

Reis S (2008) Analyzing land use/land cover changes using remote sensing and GIS in Rize, North-East Turkey. Sensors 8(10): 6188–6202. https://www.mdpi.com/1424-8220/8/10/6188

Şahin B (2021) Karabük-Yenice Nature Reserve Area, https://dogadakiler.com/Gezilesi-Yerler/karabuk-yenice-doga-koruma-alanlari/, [accessed on 24/05/2021]

Salem M, Tsurusaki N, Divigalpitiya P (2020) Land use/land cover change detection and urban sprawl in the peri-urban area of greater Cairo since the Egyptian revolution of 2011. J Land Use Sci 15(5):592–606. https://doi.org/10.1080/1747423X.2020.1765425

Sarma PK, Lahkar BP, Ghosh S, Rabha A, Das JP, Nath NK, Dey S, Brahma N (2008) Land-use and land-cover change and future implication analysis in Manas National Park, India using multitemporal satellite data. Curr Sci 95(2): 223–227. https://www.jstor.org/stable/24103050

Shafizadeh-Moghadam H, Minaei M, Feng Y, Pontius RG Jr (2019) GlobeLand30 maps show four times larger gross than net land change from 2000 to 2010 in Asia. Int Appl Earth Obs Geoinf 78:240–248. https://doi.org/10.1016/j.jag.2019.01.003

Singh SK, Mustak S, Srivastava PK, Szabó S, Islam T (2015) Predicting spatial and decadal LULC changes through cellular automata Markov chain models using earth observation datasets and geoinformation. Environ Process 2(1):61–78. https://doi.org/10.1007/s40710-015-0062-x

Snedecor C, Cochran M (1969) Statistical methode, 6th edn. The Iowa State Univ, Press, Iowa, USA

Song W, Liu M (2017) Farmland conversion decreases regional and national land quality in China. Land Degrad Dev 28(2):459–471. https://doi.org/10.1002/ldr.2518

Srivastava PK, Han D, Gupta M, Mukherjee S (2012) Integrated framework for monitoring groundwater pollution using a geographical information system and multivariate analysis. Hydrol Sci J 57(7):1453–1472. https://doi.org/10.1080/02626667.2012.716156

Sun X, Li G, Wang J, Wang M (2021) Quantifying the Land use and Land cover changes in the Yellow River basin while accounting for data errors based on globeland30 Maps. Land 10(1):31. https://doi.org/10.3390/land10010031

Tadese M, Kumar L, Koech R, Kogo BK (2020) Mapping of land-use/land-cover changes and its dynamics in Awash River basin using remote sensing and GIS. Remote Sens Appl: Soci Environ 19:100352. https://doi.org/10.1016/j.rsase.2020.100352

Tan L, Shao G (2015) Drone remote sensing for forestry research and practices. J For Res 26(4): 791–797. https://link.springer.com/article/https://doi.org/10.1007/s11676-015-0088-y

Tole L (2002) An estimate of forest cover extent and change in Jamaica using Landsat MSS data. Int J Remote Sens 23(1): 91–106. https://www.tandfonline.com/doi/abs/https://doi.org/10.1080/01431160010014837

TUIK (2021) Immigration Received, Given by Provinces, Net Migration and Net Migration Rate, General Population Censuses, https://data.tuik.gov.tr/Kategori/ GetKategori?p=Nufus-ve-Demografi-109 [accessed on 14/05/2021]

Twisa S, Buchroithner MF (2019) Land-use and land-cover (LULC) change detection in Wami River basin. Tanzania Land 8(9):136. https://doi.org/10.3390/land8090136

USGS (2021) United States Geological Survey (USGS) https://earthexplorer.usgs.gov/) accessed on 15.05.2021

Varga OG, Pontius RG Jr, Singh SK, Szabó S (2019) Intensity analysis and the figure of merit's components for assessment of a cellular Automata–Markov simulation model. Ecol Indic 101:933–942. https://doi.org/10.1016/j.ecolind.2019.01.057

Varol T, Yılmaz B (2006) Possibilities of utilizing GIS in determining the changes in forest areas Bartın Sökü forest operation directorate example, 4. geographic information systems, information days,13–16.09.2006, Istanbul, Turkey.

Wang T, Kazak J, Han Q, de Vries B (2019) A framework for path-dependent industrial land transition analysis using vector data. Eur Plan Stud 27(7): 1391–1412. https://www.tandfonline.com/doi/full/https://doi.org/10.1080/09654313.2019.1588852

Weng Q (2001) A remote sensing? GIS evaluation of urban expansion and its impact on surface temperature in the Zhujiang Delta. China Int J Remote Sens 22(10):1999–2014. https://doi.org/10.1080/713860788

Yang Y, Liu Y, Xu D, Zhang S (2017) Use of intensity analysis to measure land use changes from 1932 to 2005 in Zhenlai County. Northeast China Chin Geogr Sci 27(3):441–455. https://doi.org/10.1007/s11769-017-0876-8

Zaehringer JG, Eckert S, Messerli P (2015) Revealing regional deforestation dynamics in North-Eastern madagascar—insights from multi-temporal land cover change analysis. Land 4(2):454–474. https://doi.org/10.3390/land4020454

Zeng Y, Huang W, Liu M, Zhang H, Zou B (2010) Fusion of satellite images in urban area: assessing the quality of resulting images. In 2010 18th international conference on geoinformatics, (pp. 1–4), June 2010. IEEE.

Zhou P, Huang J, Pontius RG, Hong H (2014) Land classification and change intensity analysis in a coastal watershed of Southeast China. Sensors 14(7):11640–11658. https://doi.org/10.3390/s140711640